EFFECTS OF LAND USE CHANGE ON SOIL EROSION IN THE UPPER-MIDDLE BASIN OF MIRA RIVER IN ANDEAN-ECUADOR

Paúl Arias-Muñoz[1, 2], Miguel Ángel Saz[2, 3], Severino Escolano[2, 3]

1 Universidad Técnica del Norte, Ibarra-Ecuador, Facultad de Ingeniería en Ciencias Agropecuarias y Ambientales, Carrera de Recursos Naturales Renovables, email: dparias@utn.edu.ec

2 Universidad de Zaragoza, España, Departamento de Geografía y Ordenación del Territorio

3 Universidad de Zaragoza, España, Instituto Universitario de Ciencias Ambientales de Aragón

Abstract: This study examined the effects of land use change on the potential of soil loss in the upper-middle basin of the Mira River in Andean Ecuador in the years 1995 and 2017 and by the future year 2030. The study is based on modeling soil erosion and LULC change by applying GIS and remote sensing. RUSLE equation was used to quantify soil erosion rates, and CA-Markov chain analysis was implemented to forecast the LULC change for the 2030 year. The results showed that the annual average soil erosion passed from 14.72 t/ha/year to 32.78 t/ha/year and will probably achieve 41.01 t/ha/year by 2030. Between 1996-2018 and 2018-2030, the conversion and probable conversion towards bare soils and crops led to soil loss and unsustainable production rates by far greater than >10 t/ha/year. Some recommended measures to prevent soil erosion include restoring areas with scarce vegetation cover and integrating soil conservation measures with tillage practices and grazing activities. Practices such as strip cropping, contour cropping, building terraces on sloping areas, grazing regulation, or implying deep tillage and soil amendments are recommended.

Keywords: land use change, land cover, erosion soil, RUSLE, Andean

1 INTRODUCTION

In recent years, land use change and land cover (LULC) have been the main risk drivers because they can cause system perturbations and lead to global environmental changes (Anand et al., 2018). LUCC can cause impacts ranging from changes in soil structure (Zhong et al., 2019), agricultural and urban expansion (Pullanikkatil et al., 2016), hydrology (Martínez-Retureta et al., 2020), biodiversity (Hansen et al., 2012) to increased susceptibility to extreme events such as floods, landslides, erosion (Pisano et al., 2017; Borrelli et al., 2020). Losses of vegetation cover can lead to the formation of soil seals, which causes increased runoff and erosion in the early stages of seal formation (Singer and Le Bissonnais, 1998). The soil seal formation is most common in humid regions by the raindrop effect and by sediment deposition from the infiltration of sediment-laden overland flow (Moss, 1991; Holz et al., 2015). Different models have been developed to calculate the spatial differences in erosion rates, which result mainly from differences in topography and land covers (Wischmeier and Smith, 1978; Skidmore, 1986; Obiahu and Elias, 2020).

Land use changes affect the intensity of runoff and soil erosion (Ozsahin et al., 2018; Yang and Lu, 2018; Martínez-Retureta et al., 2020). Land cover changes towards more anthropogenic land cover cause changes in soil physical and chemical properties, as well as in the variation of soil erosion rates (Li et al., 2020). Authors such as (Borrelli et al., 2017) found that globally between 2001 and 2012, soil erosion rates increased by about 0.6 million tons per year, which they attributed 80% to the increase in crops. Consequently, the presence of crops implies a direct relationship with increased erosion (Alkharabsheh et al., 2013; Vijith et al., 2018; Devátý et al., 2019; Viteri-Salazar and Toledo, 2020). This background makes the route to save natural vegetation a tool to keep erosion rates under control (Woo et al., 1997; La Manna et al., 2021; Vanacker et al., 2022).

In Ecuador, erosion is the leading cause of soil degradation (De Noni and Trujillo, 1986a). Anthropogenic factors that increase erosion range from deforestation, intensive soil use, expansion of smallholdings, and poor agricultural technological development (Espinosa, 2014). Agricultural expansion shaped the spatial organization of the country, mainly in the foothills of the Andes, the coastal lowlands of Ecuador, and the Amazon region (Barbieri et al., 2005; Stadel, 2005; Curatola Fernández et al., 2015; Viteri-Salazar and Toledo, 2020). Although agricultural development has led to population growth in Ecuador through colonization and the development of new settlements, it also is one of the causes of biodiversity loss and environmental degradation (Jokisch, 2002; Haro-Carrión and Southworth, 2018). Agricultural expansion, both rainfed and irrigated, towards the foothills of the Andes, in addition to colonization and agricultural expansion into the high Andean zones, has also caused an increase in erosion in these sectors (De Noni and Trujillo, 1986b; Viteri-Salazar and Toledo, 2020). By the 1980s, 60% of the country's area was affected by erosion in the high Andean zones (De Noni and Trujillo, 1986b).

The Mira River basin is a binational hydrography located between Ecuador and Colombia. The basin is distributed mainly through the high Andean regions. In the upper-middle section, located in the Ecuadorian sector, the population has shown moderate growth, with a projected total of 647,598 inhabitants by 2020 (Instituto Nacional de Estadística y Censos, 2010). The population increase within the watershed, along with economic development, has led to an increase in the demand for resources and changes in the consumption patterns of the inhabitants, generating the growth of various economic activities such as livestock, agriculture, mining, and forestry.

These activities have been developing in unsustainable management, causing decreased vegetation cover, increased urban and rural areas, and increased exposure to risks such as erosion. (Gonzalez et al., 2018) determined that 22 and 40 tons per hectare are lost annually in the middle-upper section of the Mira River basin. Despite these soil loss rates, there is no evidence of the implementation of soil conservation techniques during and after harvest or pasture management in the watershed (CISPDR, 2016). There is no evidence of a permanent abandonment of rural agricultural sectors and its impact on soil erosion. Consequently, assessing the temporal dynamics of LULC change and its effects on erosion risk allows decision-making for the sustainable use of natural resources and the efficient use of soil covers.

In this study, the main aim was to determine the effects of land use change on the potential of soil loss in the upper-middle basin of the Mira River in Andean Ecuador. It was aimed firstly to identify and predict the changes in LULC classes over time, secondly to obtain the temporal variation and spatial distribution of soil erosion by utilizing temporal LULC change, and finally to assess the effects of changes in land use on soil erosion. The approach is based on modeling soil erosion and LULC change by applying GIS and remote sensing. RUSLE equation was used to quantify soil erosion rates, and CA-Markov chain analysis was implemented to forecast the LULC change for the 2030 year. The employment of RUSLE and CA-Markov in a mountainous area is a novel contribution of this study in an Ecuadorian Andean region.

2 MATERIALS AND METHODS

2.1 Study area

The research is limited to the section upper-middle basin of the Mira River located in the Ecuador Nor-West Region, between 78°26′44″ and 77°46′01″ longitude West and between 0°11′09″ to 0°52′25″ of latitude North. The upper-middle basin area is 5320.87 km^2 with a varied relief, characterized by valleys and mountains in its highest regions. The relief descends gradually as a hillside until it flows into the Pacific Ocean. The climate is characterized by a mean temperature of 21.7° and a mean annual precipitation of 1152 mm. The annual precipitation varies between 500 mm and 2900 mm (Instituto Nacional de Meteorología e Hidrología, 2005) (Figure 1).

2.2 Methodology

Acquisition and image processing

According to the project, multispectral satellite images of the group of satellites were used by the satellite group Landsat Thematic Mapper (TM) and Sentinel-2. For 1996, 2007, and 2018, the images captured by the Landsat 5 TM (row 10/routes 59 and 60 of the WRS-2) on July 8th, 1996, Landsat 7 ETM (row 10/routes 59 and 60 del WRS-2) on December 6th, 2007, and Sentinel-2B with dates on August 5 and

24th, 2018, were used respectively. In each image, a preprocessing was performed, including geometric, radiometric, and atmospheric corrections. These data were georeferenced to the study area using the reference system WGS84 projecting UTM, zone 17 South. The study area was extracted from the acquired satellite images using the watershed boundary generated. This boundary was generated in a GIS environment. The information used was river data and the space Shuttle Radar Terrain Mission (SRTM) digital elevation model (DEM) product, with a 30 m spatial resolution (http://srtm.csi.cgiar.org/). Due to Sentinel satellite images having a different spatial resolution to images of Landsat, these images were resampled using the nearest resample method to keep the images' resolution uniformity (Astola et al., 2019).

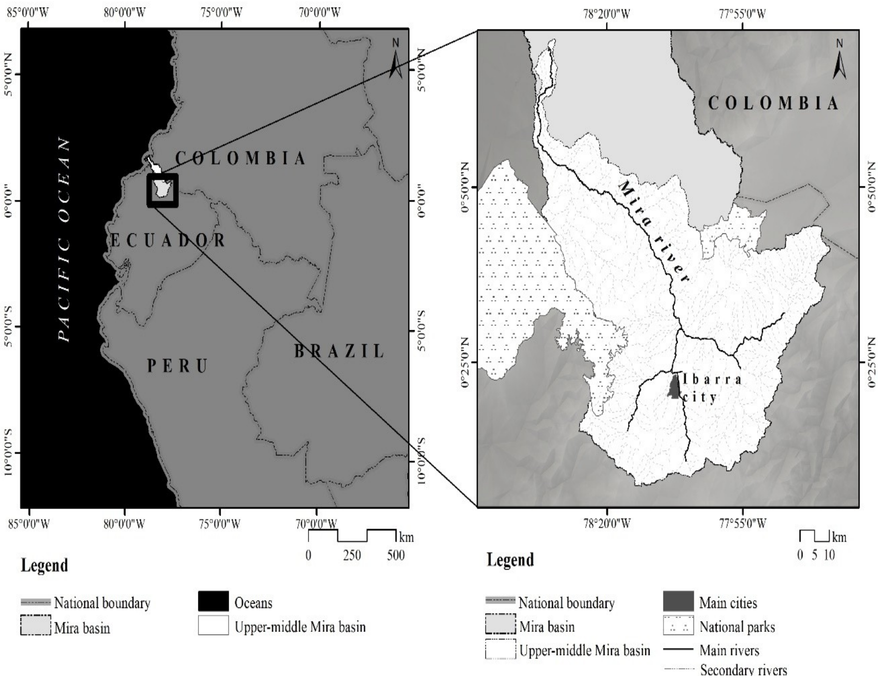

Figure 1 Map of the study area

Field data in 2018 using geospatial positioning system (GPS) records, besides information from Google Earth in 2011 and aerial photographs from 1999 taken by the Military Geographic Institute of Ecuador, were collected to prepare the land use maps using ArcGIS and "Idrissi TerrSet" software. The supervised classification technique, maximum likelihood, was applied to obtain eight land covers: forest, paramo, scrubland, crops, pastures, urban zone, bare soil, and bodies of water. The paramo is a particular ecosystem in the Andean zones of South America, located between the forest line and the perpetual snow. It is generally found at altitudes above 3500 meters above sea level, although it can vary according to latitude and the specific topography of the region (Buytaert et al., 2006). Finally, the classification accuracy assessment was performed for each LULC map by applying the matrix confusion and the corresponding Cohen's Kappa index using the collected GCPs (Ground Control Points) (Arévalo-Morocho et al., 2023).

Analysis of the change of LULC and prediction of its future dynamic to 2030

The CA-Markov model is a hybrid model used to predict and show a better simulation of quantitative and spatial change of the LULC. The hybrid model allows the forecast of changes generated by Markov analysis from observed rates of change in one period (T1 to T2) to the simulation period (T2 to T3) to have a spatial dimension using automata cells (ACs) (Eastman, 2006). The prediction of future LULC dynamics to the 2030 year in the Mira basin was performed by using the software TerrSeT 2020. For this purpose:

a. It is determined variables and maps suitable based on an evaluation of multiple criteria.
b. The matrix of transparency and the matrix of the transition state probability are generated using the Markov model.
c. The LCM (Land Change Modeler) integrated into the TerrSet software was used to predict the future LULC for 2030.

Suitability maps show the suitability of converting a land use/land cover to another one by each map cell (Figure 2). The suitability maps were developed following the inductive approach, MCE, which consists of converting a set of weighted factors and constraints into maps using fuzzy membership functions (Cabral and Zamyatin, 2009). These maps were elaborated on an empirical basis considering the environmental factors that are significant for land use change or that will generate change restrictions in a region (Eastman, 2006; Eastman and Toledano, 2018) The change factors can be static or dynamic. For the study, the static factors identified were elevation and slope (derivate of DEM-SRTM). The statics variable used the distances to the communication and distance routes to urban areas. The only restrictive variable was the protected natural areas to keep the coverage of these spaces without changes inside the projection. These protected natural areas are zones that will keep intact over time since being protected by current environmental regulations. Distance is an indicator of accessibility and a critical factor in expanding urban spaces (Leta et al., 2021). As a complement to this last is found the distance to the urban zones because the closer these spaces are, the easier it is to convert coverage close to an urban use (Gharaibeh et al., 2020). The elevation and the slope are topographic factors that affect the change of LULC because of the profit of urban and agricultural zones, which are concentrated mainly on relatively flat slopes, and deforestation decreases with the increasing gradient of slopes (Wang et al., 2021).

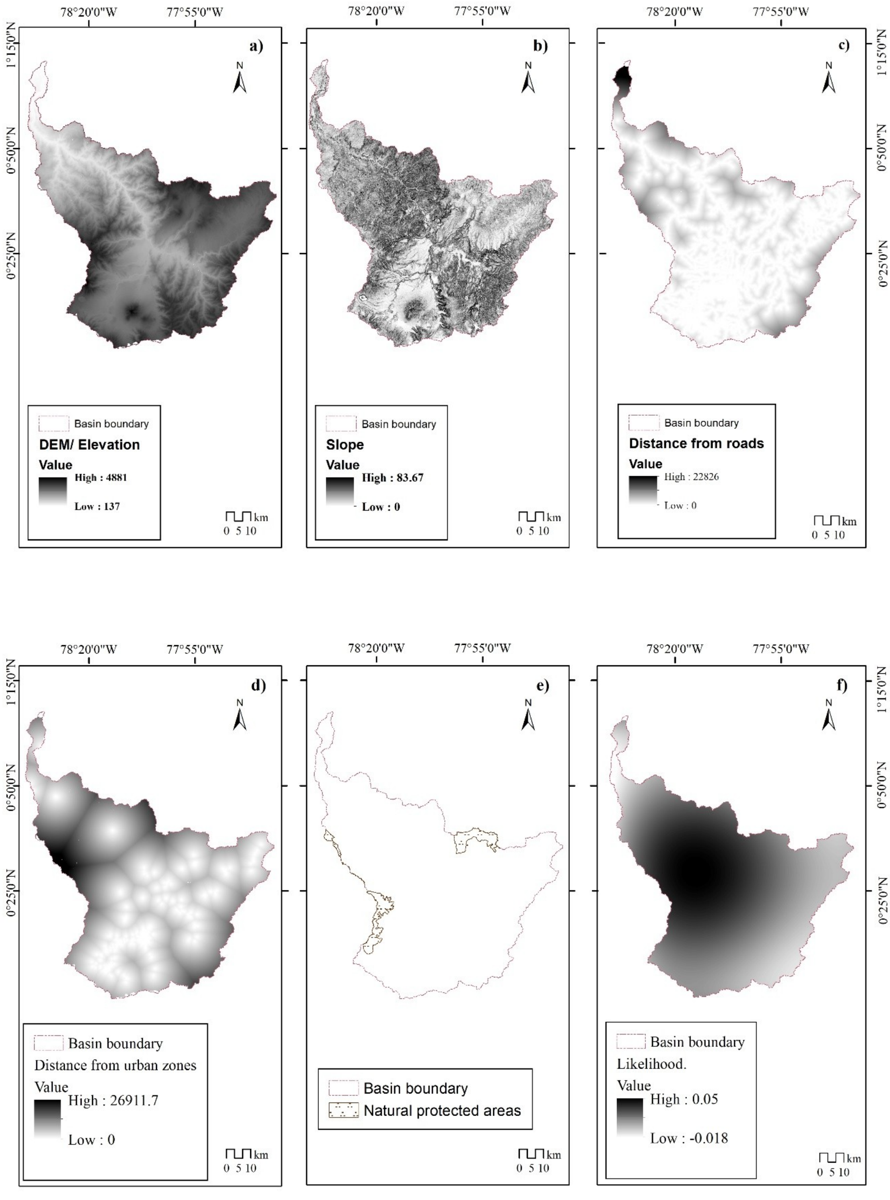

Figure 2 Suitable maps. a) Elevation, b) Slope, c) Distances to the roads of communication, d) Distance to the urban zones, e) Protected natural areas, f) Map of authenticity. Source: National Planning Secretary of Ecuador (2013), own elaboration

In the second place, the percentages of changes that occurred in LUCL between 1996-2007 and 1996-2018 were determined using the Earth Change Modeler of the software TerrSET 2020. The possible factors causing the change in land use are identified through the test of V of Cramer in TerrSET software. These results are used to generate the matrix of the probability of transition of the classes LULC and the transition potential maps. This pixel transition analysis did not include areas smaller than 100 hectares. In the Land Change Modeler integrated into the TerrSET software, land use coverages for 1996 and 2007 were entered, and the potential transition map for 2018 was simulated using the MLP tool. The LULC 2018 projection was validated with the Ground Control Points taken by the 2018 year. The obtained model was compared with the real data captured, as recommended by Žoncová and Masný (2022). Once the prediction has been validated, the future scenario for 2030 was simulated, using 1996 as time one and 2018 as time two.

Revised Universal Soil Loss Equation

Soil water erosion was quantified using the universal soil loss equation (Equation 1), RUSLE (Renard, 1997).

$$A = R * K * LS * C * P \quad , \tag{1}$$

where *A* is the annual soil loss (t/ha/year); *R* is the rainfall erosivity (MJ mm/ ha/ year); *K* is the soil erodibility (t h ha/ ha MJ mm); *LS* is the topographic factor representing the length and steepness of the slope (dimensionless); *C* is the cover management (dimensionless), and the *P* factor represents the conservation practices (dimensionless).

The erosion factor R measures the effect of rainfall intensity on soil erosion. An average of 20 to 25 years or even longer of data is recommended to calculate the R factor (Wischmeier and Smith, 1978). The R factor was calculated by applying Equation (2) proposed by (Wischmeier and Smith, 1978) and later modified by (Arnoldus, 1980).

$$Factor\ R = \sum_{i=1}^{12} 1{,}735 * 10^{\left(1{,}5 \log 10\left(\frac{p_i^2}{P}\right) - 0{,}08188\right)} \quad , \tag{2}$$

where *R* (x, y) is the R factor (MJ mm ha-1 h-1 yr-1) in cell size (x, y), p_i is monthly precipitation (mm), and *p* is annual precipitation (mm).

For the present study, historical precipitation WorldClim records for 1970-2000 years in TIF format were used (Fick and Hijmans, 2017). A statistical downscaling was performed to obtain a raster with a spatial resolution of 30 meters. The predictor variables were latitude and longitude. This process was performed as recommended by (Arias-Muñoz et al., 2023), who found that between the data obtained from the statistical downscaling for the study area and data from the meteorological stations, there is a correlation of R2=0.91, a BIAS=1.03 and a root mean square error RMSE = 219.85 mm.

The *K* factor represents the susceptibility to soil erodibility (Wischmeier and Smith, 1978). The following equation was used for the calculation of the *K* factor.

$$K = 27{,}66\, X\, m^{1{,}14}\, x\, 10^{-8} (12 - a) + 0{,}0043 (b - 2) + 0{,}0033 (c - 3) \quad , \tag{3}$$

where m = (silt (%) + very fine sand (%) *(100 – clay (%)); a is organic matter (%); b is structure code; c is permeability code. The information was obtained from the spatial database of soil texture, organic matter, and permeability at a scale of 1:25,000 developed by the (Military Geographic Institute of Ecuador, 2022), and soil properties were interpreted using the monogram.

The topographic factor (LS) represents the combined effect of slope steepness (S) and slope length factor (L) on soil loss (Zhang et al., 2017). The LS factor was calculated using LS-Tool software (Zhang et al., 2017) from the 30-meter spatial resolution DEM-SRTM elevation model.

The cover management factor (C) corresponds to the relationship between soil loss and vegetation types and can be qualitatively classified according to vegetation types (Wischmeier and Smith, 1978). In this study, C factor values for the land cover were allocated according to the determined by (Arias-Muñoz et al., 2023) for the Mira basin (Table 1).

Table 1 Values of Factor *C* by land cover

Land cover	Factor C
Forest	0,01
Scrubland	0,035
Paramo	0,040
Pasture	0,037
Crops	0,35
Bare soil	0,43

Source: Own research based on Arias-Muñoz et al. (2023)

Factor (P) vary between zero (0) and one (1). The first value represents the effective presence of conservation practices, and the second value represents the non-existence of conservation practices (Vijith et al., 2018). Finally, Figure 3 shows the methodology process.

3 RESULTS

3.1 Land use change

The supervised classification of coverage and using the watershed Mira River obtained a Kappa rate of 0.88. Figure 4 presents the LULC maps and their changes in 1996 and 2018 in the upper-middle basin of the Mira River. By 2018, the forest surface of 195367.29 ha had decreased by 20.04% since 1996. The scrublands were reduced even more than the woods, losing 67.36% of their area. On the contrary, bare soils and crops are the most expanded, increasing their extension by 196.54%

and 165.21%, respectively. The urban center also is incremented and almost duplicates its surface, passing from 2403.71 ha in 1996 to 4607.87 ha in 2018 (Table 2). During this period, other coverage, like pastures and paramos, decreased their surfaces by 13.83% and 2.26%, respectively. However, this decrease is relatively lower than the rest of the coverages. In summary, land cover changes between 1996-2018 in the watershed of Mira River show a clear tendency of profit in anthropic and loss in natural cover.

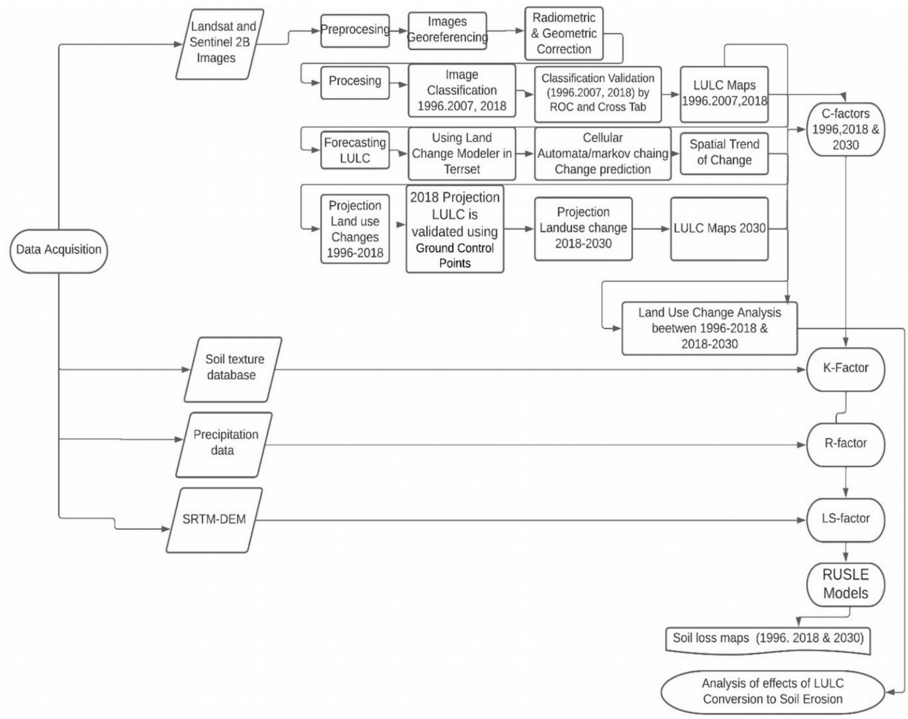

Figure 3 Methodology process, own elaboration

3.2 Prediction of LULC changes based on the CA–Markov model

Baseline, the model created for the forecast of the changes of LULC of the watershed Mira River, obtained a value of 0.72 of Kappa rate for the model project of 2018 concerning the map generated with satellite images. It is evidenced that the pathway used in this study was valid when carrying out the prediction for the year 2030.

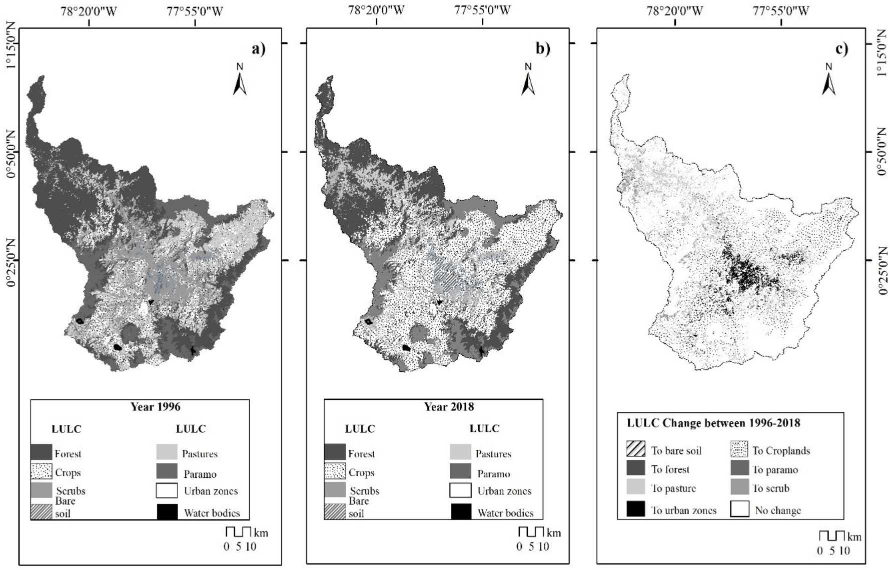

Figure 4 LULC maps and their changes in 1996 and 2018 in the upper-middle basin of the Mira River. a) map of LUCL of the year 1996, b) LULC of the year 2018, c) transition of the changes of land cover between 1996 and 2018. Source: (Earth Resources Observation and Science Center, 2022), own elaboration

Table 2 Land use change from 1996 to 2018

Covertures	1996 (ha)	2018 (ha)	Net change (ha)	Net change (%)
Bare soil	5195.63	15407.14	10211.51	196.54
Crops	69917.61	185425.52	115507.91	165.21
Urban zone	2403.71	4607.87	2204.16	91.69
Water bodies	1671.35	1667.28	-4.07	-0.23
Paramo	67206.09	65685.79	-1520.3	-2.26
Pastures	76523.13	65934.96	-10588.17	-13.83
Forest	195367.29	156219.42	-39147.87	-20.04
Scrubs	113802.23	37139.12	-76663.11	-67.36

Source: (Earth Resources Observation and Science Center, 2022), own elaboration

The LULC scenario forecasted for 2030 showed a gain in anthropic coverture and a loss in natural coverage as in 1996-2018 (Table 3, Figure 5). This projection indicates that urban centers and crop areas are the only coverage that will present

Table 3 Changes in the land cover from 2018 to 2030

Covertures	2018 (ha)	2030 (ha)	Net change (ha)	Net change (%)
Urban zone	4607.87	7001.71	2393.84	51.95
Crops	185425.52	216782.34	31356.82	16.91
Bare soil	15407.14	15405.25	-1.89	-0.01
Scrubs	113802.23	37130.34	-76671.89	-0.02
Water bodies	1667.28	1654.87	-12.41	-0.73
Forest	156219.42	145537.36	-10682.06	-6.84
Pastures	65934.96	56367.17	-9567.79	-14.51
Paramo	65685.79	52208.06	-13477.73	-20.52

Source: (Earth Resources Observation and Science Center, 2022)

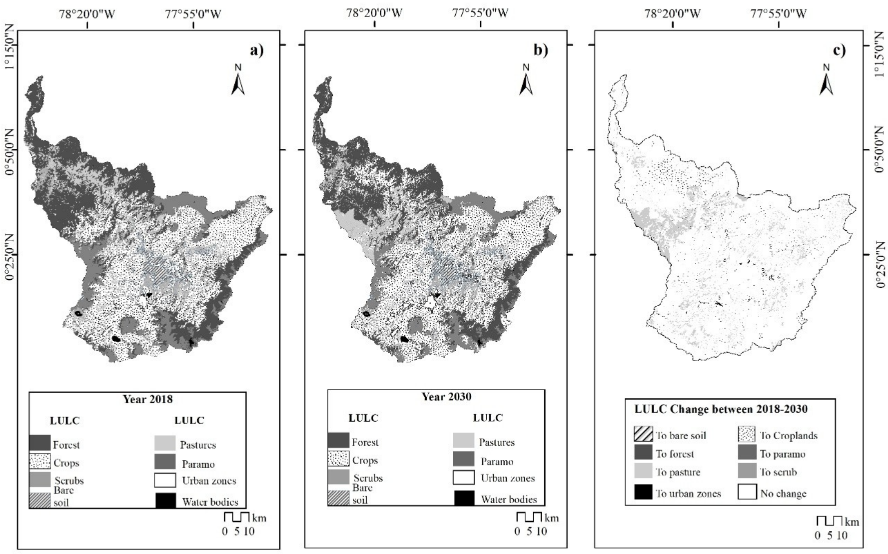

Figure 5 LULC maps and their projected changes from 2018 to 2030 in the upper-middle basin of the Mira River. a) LULC map of the year 2018, b) LULC of the projected map to the year 2030, c) transition of the land cover changes projected between 2018 and 2030. Source: (Earth Resources Observation and Science Center, 2022), own elaboration

growth in 2030. The coverage changes in bare soils and the scrublands are minimal compared to 1996-2018. Likewise, the projection for 2018-2030 evidenced a reduction of 20.52% for the paramo, which was higher than the 2.26% observed in 1996-

2018. On the contrary, the forest reduction will only be 6.84% compared to the 20.04% observed in 1996-2018.

3.3 RUSLE Factors

RUSLE factors determined in this study are presented in Figure 6. The rainfall erosivity (R-factor) values ranged from 208.905 to 1,954.9 MJ mm/h ha year (mean of 550.47 MJ mm/h ha year) (Figure 6a). The soil erodibility (K-factor) values ranged from 0 t ha h/ha MJ mm to 0.11 t ha h/ha MJ mm (Figure 6b). The LS factor values ranged from 0.01 in the flat sectors of the watershed to 67.5 in sectors with slopes higher than the average slope (Figure 6c). The cover management factor (C-factor) present values were in the range of 0 to 1. Generally, the lowest values are present in the western and southwestern parts of the study area, where the presence of forests characterizes the sectors. The highest values are characterized by bare soil. This last cover increases in the middle section of the basin, mainly in the eastern sectors of the city of Ibarra. The C values vary between the years 1996, 2018, and 2030 (Figure 6d-f). Finally, conservation practices were not identified in the basin, so the P-factor was assigned a value of 1.

3.4 Spatial and temporally soil erosion

In 1996 the annual average soil erosion was 14.72 t/ha/year, and in 2018 the mean soil loss increased to 32.78 t/ha/year. By 2030, soil erosion will be 41.01 t/ha/year. Figure 7 shows the spatial distribution of soil erosion intensity for each year. The annual average soil erosion rates between 1996 and 2018 increased by 123%, which means a rate of 5.57% per year. In 2030, an increase in erosion of 25% is expected, which means a rate of 2.09% per year since 2018. The maximum erosion rate increased from 802.79 t/ha/year in 1996 to 812.3 t/ha/year in 2018 (Figure 7a-b). By 2030, however, soil erosion will grow to 2590.98 t/ha/year (Figure 7c).

Contribution of LULC Conversions to Soil Erosion

Although they are not the cover conversions that occupy more surface area for the year 2018, conversion from forests to crops leads to soil loss with average erosion rates of 119.24 t/ha/year. The major conversions of LULC were 55255.47 ha of pastures and 53339.36 ha of scrubs to crops, losing less soil with a mean of 62.41 t/ha/year and 70.49 t/ha/year, respectively. Other conversions exceed 10 t/ha/year of soil loss, considered the sustainable threshold for erosion in tropical areas. There are land conversions that do not exceed, which means either exits vegetation conservation or the presence of water bodies or urban areas (Figure 8a-g and Table 4).

Likewise, quantities of soil loss through erosion observed will follow a similar trend to LULC conversions until 2030 (Table 4). For the future, the highest soil erosion rate is expected in the conversion of 40998.55 ha of pastures to crops. In addition, transitions of paramo to crops with 8467.99 ha, and forests to crops with 7696.99 ha, will show a mean erosion rate of 99.90 t/ha/year and 80.45 t/ha/year, respectively (Table 4 and Figure 9a-g). While in the future, areas that either will convert to urban or will pass from one will keep mean soil erosion lower by 10/ha/year, as will areas that will revert to paramo.

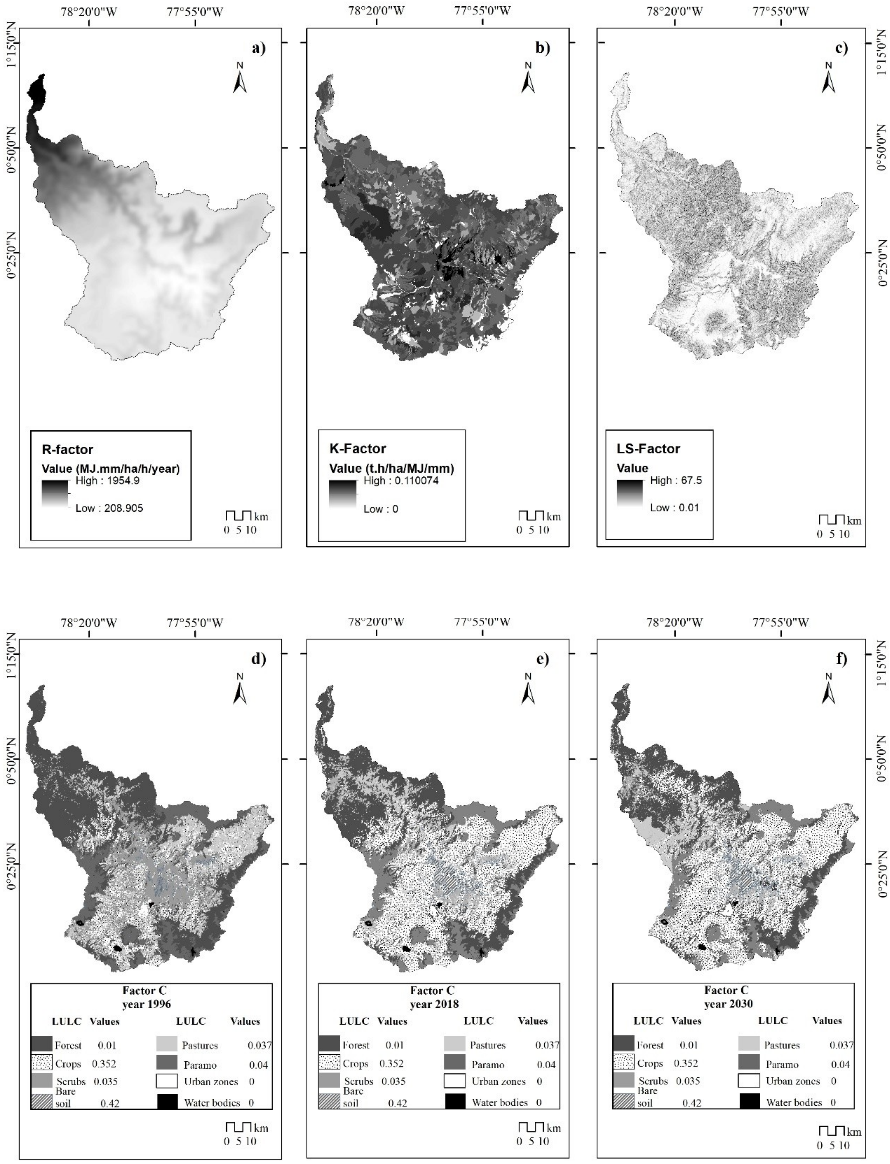

Figure 6 RUSLE Factors. a) R-factor, b) K-Factor, c) LS-Factor, d) C-Factor by 1996, e) C-Factor by 2018, f) C-Factor by 2030. Source: (Earth Resources Observation and Science Center, 2022), Military Geographic Institute of Ecuador (2022), Fick and Hijmans, (2017), Zhang et al. (2017), own elaboration

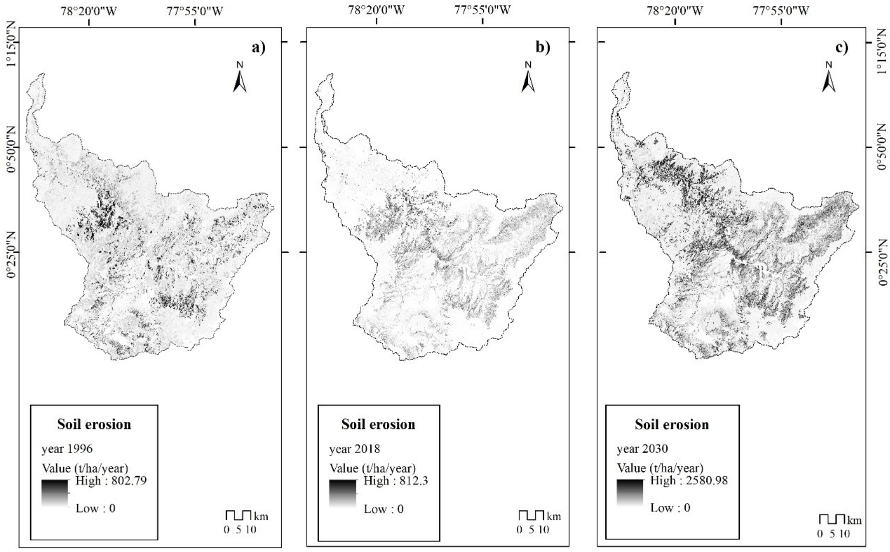

Figure 7 Soil erosion a) 1996, b) 2018, c) 2030. Source: Own elaboration in base of Rusle Equation (Renard, 1997)

4 DISCUSSION

In this research, we examined soil erosion in the Mira watershed using the RUSLE model in a GIS environment. The study showed that the spatial distribution of rainfall- erosivity in the watershed was consistent with the amount of precipitation received per sector. The consensus is that precipitation is the principal climatic agent in erosive processes since the main conditioning factors are soil cover and surface flow (Mulligan, 1998). Erodibility in the watershed presents a range between 0 to 0.11 t/ha/MJ-1mm-1 ha-1, a variation very similar to that found in other mountain watersheds in Andes Mountains (Ochoa-Cueva et al., 2015; Correa et al., 2016). Erodibility is severe when it presents values higher than 0.10 t ha h/ha MJ mm (Ramírez et al., 2009). The zones with severe erodibility found present silty soils (0.05-0.002 mm), clay loam (< 0.002 mm), and on average, 3% organic matter. (Evans, 1980) mentions that soils with less than 3.5% organic matter are considered erodible, and (Kumar and Kushwaha, 2013) notes that soil erodibility increases as soil texture becomes finer. Therefore, soils are very vulnerable to erosion in heavy runoff because they have low infiltration and stability (Kogo et al., 2020).

The erosion ranges between 1996 and 2018 found in the watershed, ranging from 0 to a maximum of 812.30 t/ha/year, are higher compared to other parts of the world. Even the expected maximum erosion rate of 2580.90 will exceed the current maximum rates in other regions. In China, soil erosion varies between 0.1-360 ton/ha/year; in the USA, it varies between 0.03-170 ton/ha/year; in India, it varies

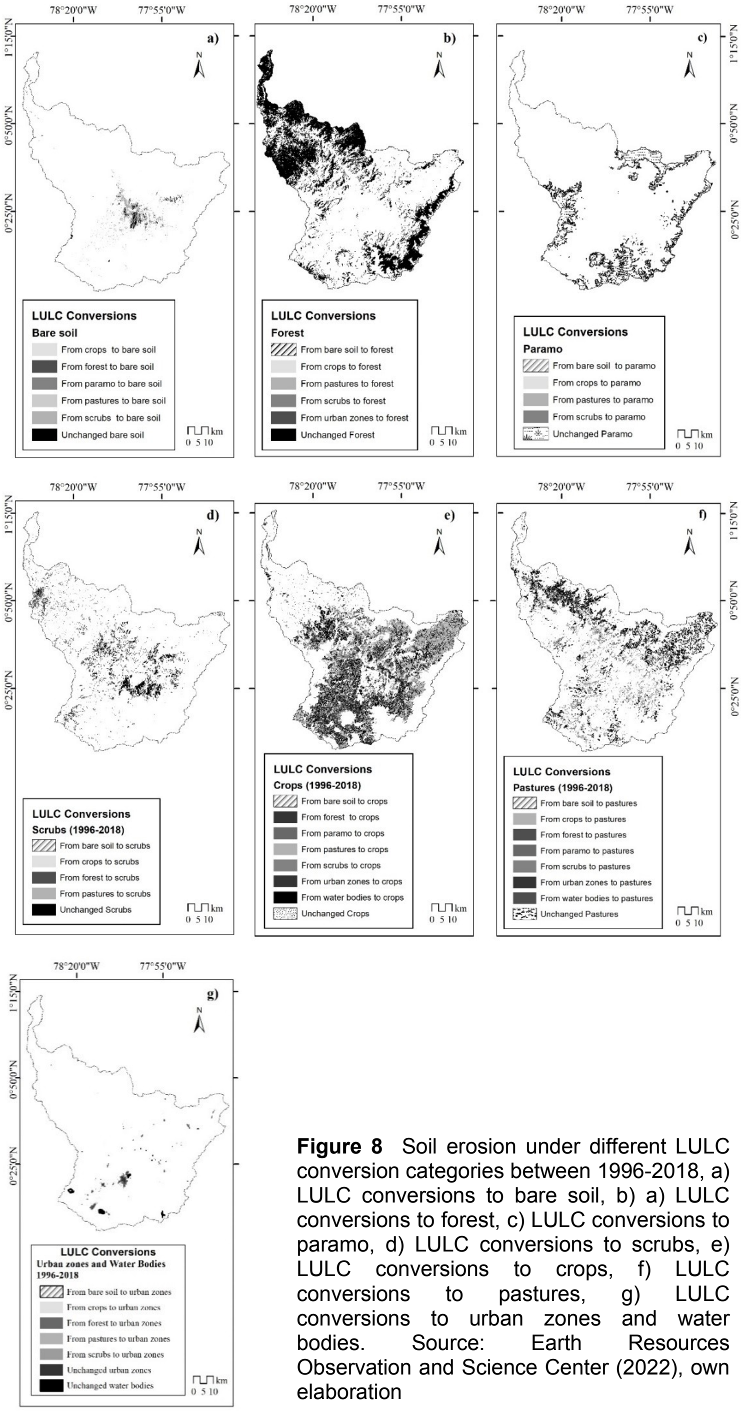

Figure 8 Soil erosion under different LULC conversion categories between 1996-2018, a) LULC conversions to bare soil, b) a) LULC conversions to forest, c) LULC conversions to paramo, d) LULC conversions to scrubs, e) LULC conversions to crops, f) LULC conversions to pastures, g) LULC conversions to urban zones and water bodies. Source: Earth Resources Observation and Science Center (2022), own elaboration

Table 4 Soil erosion under different under different LULC conversion categories

LULC Conversions	Years: 1996-2018		Years 2018-2030	
	Area (ha)	Mean Soil Erosion (t/ha/year)	Area (ha)	Mean Soil Erosion (t/ha/year)
From forest to crops	16473.43	119.24	3413.87	80.45
From scrubs to bare soil	10420.18	83.14	0	0
From forest to bare soil	54.69	73.58	0	0
Unchanged Bare soil	3628.2	72.55	15372.35	81.79
From scrubs to crops	53339.37	70.49	135.81	94.21
From pastures to crops	55255.47	62.41	40998.56	150.08
Unchanged Crops	58966.39	60.03	163740.04	64.2
From bare soil to crops	1293.23	52.53	25.55	45.49
From paramo to crops	79.13	50.82	8468	98.9
From crops to bare soil	921.63	40.96	23.26	43.22
From crops to forest	226.93	39.75	142.9	7.02
From pastures to scrubs	70.65	31.63	44.57	8.77
From bare soil to scrubs	21.72	29.22	0	0
From paramo to bare soil	17.22	27.47	0.53	121.25
From pastures to bare soil	365.24	26.86	9.1	71.63
From scrubs to paramo	54.08	25.61	0.41	7.82
From pastures to forest	246.48	24.41	53.36	7.28
From bare soil to forest	3.94	23.94	0	0
From crops to paramo	29.17	23.24	10.39	7.45
From pastures to paramo	54.83	22.43	11.74	8.12
From forest to pastures	13153.37	22.13	7696.99	16.36
Unchanged Pastures	20412.05	21.45	24816.59	9.39
From crops to scrubs	160.98	20.83	70.26	10.7
From scrubs to forest	592.16	20.46	3.46	6.86
From forest to scrubs	10522.29	18.07	8.86	12.93
From crops to pastures	8127.76	17.78	19056.82	15.96
From scrubs to pastures	24062.57	17.75	19.88	12.83

From paramo to pastures	46.81	15.08	4770.17	8.09
Unchanged Scrubs	24846.87	14.7	36977.83	11.62
From paramo to scrubs	1516.63	10.23	22.95	11.26
From bare soil to pastures	130.58	10.12	1.01	3.43
From urban zones to crops	14.49	9.01	0.08	0
Unchanged Paramo	65546.06	8.77	52142.26	7.87
From bare soil to paramo	1.65	8.4	0.18	8.57
Unchanged Forest	155149.66	6.36	145055.75	8.39
From water bodies to crops	4	5.74	0.43	0.05
From urban zones to pastures	1.51	4.32	0.14	0.01
From pastures to urban zones	118.42	3.06	1.03	0
From forest to urban zones	13.87	1.69	0.87	0
From scrubs to urban zones	487	1.5	1.73	0
From crops to urban zones	1484.75	0.71	2381.85	0
From bare soil to urban zones	116.33	0.57	8.05	0
Unchanged Urban zones	2387.5	0	4607.64	0
Unchanged Water bodies	1667.28	0	1655.41	0
From forest to paramo	0	0	43.08	9.19
From paramo to forest	0	0	281.88	5.16
From urban zones to forest	0.25	0	0	0
From water bodies to pastures	0.32	0	5.56	0
From water bodies to scrubs	0	0	5.88	0.02

Source: Own elaboration in base of Rusle Equation (Renard, 1997) and information from (Earth Resources Observation and Science Center, 2022)

between 0.5-185 ton/ha/year; in Australia, it varies between 0-150 ton/ha/year (Morgan, 2009) and in Europe, it is lower by varying between 0.5 and 325 ton/ha/year (Maetens et al., 2012). In Africa, erosion has also been estimated to be lower by fluctuating between 10.8 and 146 tons/ha/year (Stocking, 1984). The erosion found is also very different from other mountainous areas. In the case of Nepal, the soil erosion rate ranges between 0.5 and 185 tons/ha/year (Koirala et al., 2019), and the Sierra de Manantlán Biosphere Reserve in Mexico fluctuates between 0 and 100 tons/ha/ha/year (Millward and Mersey, 1999). In the Andes, erosion varies similarly.

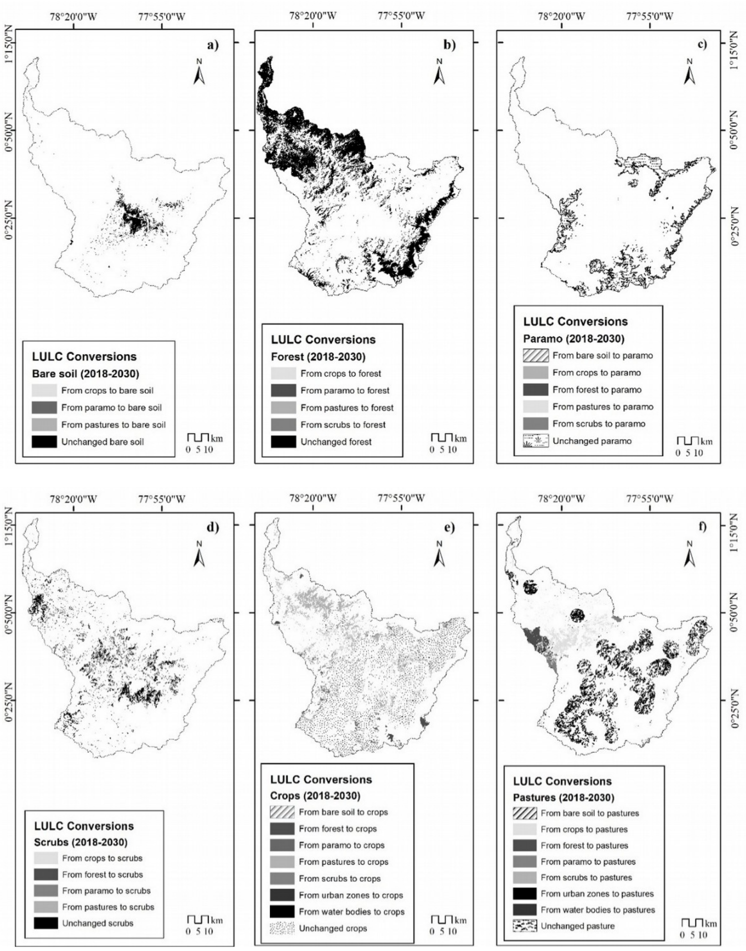

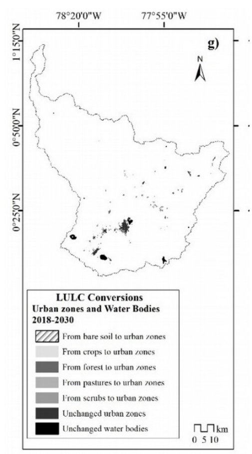

Figure 9 Soil erosion under different LULC conversion categories between 2018-2030, a) LULC conversions to bare soil, b) a) LULC conversions to forest, c) LULC conversions to paramo, d) LULC conversions to scrubs, e) LULC conversions to crops, f) LULC conversions to pastures, g) LULC conversions to urban zones and water bodies. Source: Earth Resources Observation and Science Center (2022), own elaboration

Soil erosion rates range from 0.5 to 836 t/ha/year in the central Ecuadorian Andes (Harden, 1988), 1.5 -936 t/ha/year in the Andes south of Ecuador (Ochoa-Cueva et al., 2015) and 514-873.3 t/ha/year in bare soil in the Colombian Andes (Suárez de Castro and Rodríguez Grandas, 1962). This trend of leading soil loss worldwide will be maintained in the future. The maximum rate will reach 2580.98 t/ha/year, like the 2021 t/ha/year found by Ochoa-Cueva et al. (2015) in the Andes of Southern Ecuador.

The highest soil erosion rates are concentrated in the basin hills in zones with high slope lengths and steepness of more than 60°, coupled with low vegetation cover. The data demonstrated that low vegetation cover is generated by increasing deforestation, agricultural and livestock activities, and urban expansion. In addition, these zones receive higher rainfall, with mean values of more than 1000 mm. In humid tropics, the influence of cover vegetation on erosion rates reduces when annual precipitation exceeds ~2,000 mm (Avwunudiogba and Hudson, 2014). Therefore, the main determinants of erosion in Andean watersheds are first the soil cover and then the slope, as concluded by authors as (Harden, 1988).

The results revealed that soil erosion was highest in cropland and bare soils compared to paramos and forests. The reason is a cause from 1996 until 2018, farming lands and bare soils increased. During these years, 59% of the agricultural areas and 64% of the bare soils increased in areas with slopes greater than 12°. It means the expansion of human activities and degraded zones does not occur in flat zones, and continuous cultivation of lands for crop production leads to the degradation of soils. The loss of natural cover reduces the organic matter content, which affects soil stability (Barbera et al., 2012). The forest, paramo, scrub, and pasture areas are also susceptible to soil erosion, but the rate of erosion in these areas is lower than in crops and bare soils due to better soil cover.

The advance of crops to higher altitudes in Andean is caused by new flow channels that more easily transport soil particles downhill were shaped. Additionally, the presence of fallow due to cultural practices, according to (CISPDR, 2016), in the Andean basin each year reaches 30% of the total sowing area does not generate plant succession in fallow or abandoned lands, which does not reduce erosion (Harden, 2001). Another problem is overgrazing, even above 3,000 meters above sea level (m a.s.l.). According to Harden (1988) when the Andean slope soils are transformed into bare soils because of overgrazing and agricultural advancement, they become more vulnerable to wind and water erosion. In addition, the trails and unpaved roads interconnecting rural communities form runoff channels transporting sediment (Harden, 2001).

The transformation of land cover accelerated agricultural frontier expansion in the watershed. By 2030, agricultural areas will expect an increase of 16.91%. In Ecuador's inter-Andean region, it is common for agricultural expansion to occur in areas with steep slopes, increasing soil erosion and the formation of cangahua-type soils (Espinosa, 2014; Hidrobo et al., 2015). Cangahua is a soil matrix with low nitrogen and organic matter content where agriculture is impossible (Zebrowski and Vicuña, 1997).

Therefore, reducing deforestation and regulating overgrazing is necessary because these activities pave the way for advancing the agricultural frontier and increasing erosion rates. Restoration of degraded areas is another activity that will reduce soil losses. In addition, implementing appropriate tillage practices that include terraces, contour cropping, row cropping, and agroforestry practices became necessary. Evidence shows that undisturbed vegetation cover significantly retards laminar erosion and that reforestation in degraded pastures controls erosion and prevents loss of organic matter (Woo et al., 1997; La Manna et al., 2021). In the Andean region has been demonstrated that when natural vegetation is conserved and prevented from being replaced by crops, there is a positive effect on soil quality because more organic carbon is stored (Vanacker et al., 2022).

5 CONCLUSIONS

In the upper-middle basin of the Mira River, the projected land use changes between 2018-2030 will present a trend like those observed between 1996-2018. There is evidence of a decrease in natural cover, especially of forests and pastures, compared to an increase in anthropic covers, such as crop areas and urban areas. The conversion of different covers to bare soil is a dangerous trend, due to achieved 185% between the years 1996-2018. The study findings show widespread soil erosion of low to high values when existing land cover conversions, especially from natural to anthropic covers and bare soil. The effect of bare soil and crops causes increased current and future erosion. Between 1996 and 2018, the conversion from forests to crops leads to soil loss with average erosion rates, following from scrubs to bare soil and forest to bare soil. Between 2018 and 2030, the probable conversion from pastures to crops leads to soil loss, following from paramo to bare soil and scrubs to crops. These soil loss rates are unsustainable and by far greater than >10 t/ha/year, considered the sustainable threshold. However, land covers such as paramo and forests are the least prone to these losses. The other dominant causes of soil erosion in the basin are the presence of steep slopes and high precipitation. The highest soil erosion, concentrated in zones with low vegetation cover, are in the basin hills with high slope lengths and steepness of more than 60° and precipitation with mean values of more than 1000 mm. Although precipitation triggers erosion, mountain geomorphology relegates its role to the background because the main factors that generate these erosion rates in the basin are soil cover and slope. These territory conditions and land use change generate the annual average soil erosion passed from 14.72 t/ha/year to 32.78 t/ha/year and will probably achieve 41.01 t/ha/year by 2030. At the same time, the maximum soil erosion loss passed from 802.79 t/ha/year in 1996 to 812.3 t/ha/year in 2018, and by 2030 will probably increase to 2590.98 t/ha/year. These values are among the highest in the world and make the Andean basin one of the regions that lose and will lose the most soil on the planet. Therefore, it is necessary to limit deforestation and advance the agricultural frontier towards the upper areas of the watershed, mainly along steep slopes, to avoid an increase in erosion rates in the region. Restoring areas with scarce vegetation cover and integrating soil conservation measures with agricultural and grazing activities is necessary. Some measures for preventing soil erosion include the following conservation tillage practices, water conservation and management, and restoration of vegetation cover. The recommended tillage practices are strip cropping, contour cropping, and terraces on sloping areas. Grazing regulation in high altitudes is necessary to avoid increased soil erosion by overgrazing. Deep tillage and soil amendments are recommended as measures for the cangahua restoration. Afforestation and grass cover are recommended to recover degraded areas and natural vegetation. Finally, to recover eroded soil on steep slopes, suggest the program "grain for green" that replaces eroded crops on steep slopes by forests.

References

ALKHARABSHEH, M., ALEXANDRIDIS, T., BILAS, G., MISOPOLINOS, N., SILLEOS, N. 2013. Impact of Land Cover Change on Soil Erosion Hazard in Northern Jordan Using Remote Sensing and GIS. *Procedia Environmental Sciences*, 19, 912-921. DOI: 10.1016/j.proenv.2013.06.101

ANAND, J., GOSAIN, A. K., KHOSA, R. 2018. Prediction of land use changes based on Land Change Modeler and attribution of changes in the water balance of Ganga basin to land use change using the SWAT model. *Science of The Total Environment*, 644, 503-519.

ARÉVALO-MOROCHO, C., JÁCOME-AGUIRRE, G., ORTEGA-ANDRADE, S., ROSALES-ENRÍQUEZ, O., RODRÍGUEZ-ECHEVERRY, J. 2023. Evaluación del cambio del paisaje boscoso y su impacto en la distribución de Dipsas elegans en el norte de Ecuador. *Investigaciones Geográficas*, 79, 231-250. DOI: https://doi.org/10.14198/INGEO.23541

ARIAS-MUÑOZ, P., SAZ, M. A., ESCOLANO, S. 2023. Estimación de la erosión del suelo mediante el modelo RUSLE. Caso de estudio: Cuenca media alta del río Mira en los Andes de Ecuador. *Investigaciones Geográficas*, 79, 207-230. DOI: https://doi.org/10.14198/INGEO.22390

ARNOLDUS, H. 1980. An approximation of the rainfall factor in the Universal Soil Loss Equation. In De Boodt, M., Gabriels, D. (eds.), *Assessment of Erosion*. John Wiley and Sons, New York, 127-132.

ASTOLA, H., HÄME, T., SIRRO, L., MOLINIER, M., KILPI, J. 2019. Comparison of Sentinel-2 and Landsat 8 imagery for forest variable prediction in boreal region. *Remote Sensing of Environment*, 223, 257-273. DOI: 10.1016/j.rse.2019.01.019

AVWUNUDIOGBA, A., HUDSON, P. F. 2014. A Review of Soil Erosion Models with Special Reference to the needs of Humid Tropical Mountainous Environments. *European Journal of Sustainable Development*, 3, 4, 299-310. DOI: 10.14207/ejsd.2014.v3n4p299

BARBERA, V., POMA, I., GRISTINA, L., NOVARA, A., EGLI, M. 2012. Long-term cropping systems and tillage management effects on soil organic carbon stock and steady state level of C sequestration rates in a semiarid environment. *Land Degradation & Development*, 23, 1, 82-91. DOI: 10.1002/ldr.1055

BARBIERI, A. F., BILSBORROW, R. E., PAN, W. K. 2005. Farm Household Lifecycles and Land Use in the Ecuadorian Amazon. *Population and Environment*, 27, 1, 1-27. DOI: https://doi.org/10.1007/s11111-005-0013-y

BORRELLI, P., ROBINSON, D. A., FLEISCHER, L. R., LUGATO, E., BALLABIO, C., ALEWELL, C., MEUSBURGER, K., MODUGNO, S., SCHÜTT, B., FERRO, V., BAGARELLO, V., OOST, K. V., MONTANARELLA, L., PANAGOS, P. 2017. An assessment of the global impact of 21st century land use change on soil erosion. *Nature Communications,* 8, 1, 2013. DOI: 10.1038/s41467-017-02142-7

BORRELLI, P., ROBINSON, D. A., PANAGOS, P., LUGATO, E., YANG, J. E., ALEWELL, C., WUEPPER, D., MONTANARELLA, L., BALLABIO, C. 2020. Land use and climate change impacts on global soil erosion by water (2015-2070). *Proceedings of the National Academy of Sciences*, 117, 36, 21994-22001. DOI: https://doi.org/10.1073/pnas.2001403117

BUYTAERT, W., CÉLLERI, R., DE BIÈVRE, B., CISNEROS, F. 2006. *Hidrología del páramo andino: propiedades, importancia y vulnerabilidad*. Cuenca. [online] [cit. 2023-04-15]. Available at: <http://www. paramo. org/files/hidrologia_paramo. pdf>

CABRAL, P., ZAMYATIN, A. 2009. Markov processes in modeling land use and land cover changes in Sintra-Cascais, Portugal. *Dyna*, 76, 158, 191-198.

CISPDR. 2016. *Plan Hidráulico Regional de la Demarcación Hidrográfica Mira*. [Memoria]. Changjiang Institute of Survey Planning Design and Research, pp. 1-259. [online] [cit. 2023-02-15]. Available at: <http://suia.ambiente.gob.ec/files/MEMORIA%20DH%20MIRA.pdf>

CORREA, S. W., MELLO, C. R., CHOU, S. C., CURI, N., NORTON, L. D. 2016. Soil erosion risk associated with climate change at Mantaro River basin, Peruvian Andes. *CATENA*, 147, 110-124. DOI: https://doi.org/10.1016/j.catena.2016.07.003

CURATOLA FERNÁNDEZ, G., OBERMEIER, W., GERIQUE, A., LÓPEZ SANDOVAL, M., LEHNERT, L., THIES, B., BENDIX, J. 2015. Land Cover Change in the Andes of Southern Ecuador – Patterns and Drivers. *Remote Sensing*, 7, 3, 2509-2542. DOI: 10.3390/rs70302509

DE NONI, G., TRUJILLO, G. 1986a. *Degradación del suelo en el Ecuador. Principales causas y algunas reflexiones sobre la conservación de este recurso.* 383-394. [online] [cit. 2023-03-25]. Available at: <http://horizon.documentation.ird.fr/exl-doc/pleins_textes/cc-2010/26531.pdf>

DE NONI, G., TRUJILLO, G. 1986b. *La erosion actual y potencial en Ecuador: Localizacion, manifestaciones y causas. La Erosión en el Ecuador.* Documentos de Investigación, CEDIG, Quito, Ecuador, 6, 1-14. [online] [cit. 2023-03-25]. Available at: <https://horizon.documentation.ird.fr/exl-doc/pleins_textes/divers08-01/23659.pdf>

DEVÁTÝ, J., DOSTÁL, T., HÖSL, R., KRÁSA, J., STRAUSS, P. 2019. Effects of historical land use and land pattern changes on soil erosion – Case studies from Lower Austria and Central Bohemia. *Land Use Policy*, 82, 674-685. DOI: 10.1016/j.landusepol.2018.11.058

EARTH RESOURCES OBSERVATION AND SCIENCE CENTER. 2022. *EarthExplorer. USGS Science for changing world*. [online] [cit. 2023-05-30]. Available at: <https://earthexplorer.usgs.gov/

EASTMAN, J. R. 2006. *IDRISI Andes guide to GIS and image processing*. Clark University, Worcester, 328.

EASTMAN, J. R., TOLEDANO, J. 2018. A Short Presentation of the Land Change Modeler (LCM). In Camacho Olmedo, M., Paegelow, M., Mas, J. F., Escobar, F. (eds.) *Geomatic Approaches for Modeling Land Change Scenarios. Lecture Notes in Geoinformation and Cartography*. Springer, Cham. DOI: https://doi.org/10.1007/978-3-319-60801-3_36

ESPINOSA, J. 2014. La erosión en Ecuador, un problema sin resolver. *Siembra*, 1, 1, 7.

EVANS, R. 1980. Mechanics of water erosion and their spatial and temporal controls: an empirical viewpoint. In Kirkby, M. J., Morgan, R. P. C. (eds.). *Soil Erosion*. Wiley, Chichester, 109-128.

FICK, S. E., HIJMANS, R. J. 2017. WorldClim 2: New 1-km spatial resolution climate surfaces for global land areas. *International Journal of Climatology*, 37, 12, 4302-4315. DOI: 10.1002/joc.5086

GHARAIBEH, A., SHAAMALA, A., OBEIDAT, R., AL-KOFAHI, S. 2020. Improving land-use change modeling by integrating ANN with Cellular Automata-Markov Chain model. *Heliyon*, 6, 9, e05092. DOI: 10.1016/j.heliyon.2020.e05092

GONZALEZ, I. M. M., LIMAICO, D., ARCOS, C., ASTUDILLO, M. J., PANTOJA, M., AÑAZCO, M. 2018. Rehabilitación de suelos degradados mediante especies forestales en estructuras conservacionistas en la cuenca media del Río Mira, Ecuador. *II Jornadas de Investigación Científica UTN. 1 Foro de Investigación Científica "Desafíos actuales de la sociedad del conocimiento*, 195-201. [online] [cit. 2023-01-24]. Available at: <https://issuu.com/utnuniversity/docs/ebook-ii-jornadas-internacionales-u/800>

HANSEN, A. J., DEFRIES, R. S., TURNER, W. 2012. Land use change and biodiversity. En Land change science. In Gutman, G., Janetos, A. C., Justice, Ch. O., Moran, E. F., Mustard, J. F., Rindfuss, R. R., Skole, D., Turner, B. L., Cochrane, M. A. (eds.) *Land Change Science. Remote Sensing and Digital Image Processing*, vol 6., Springer, Dordrecht, 277-299. DOI: https://doi.org/10.1007/978-1-4020-2562-4_16

HARDEN, C. 1988. Mesoscale Estimation of Soil Erosion in the Rio Ambato Drainage, Ecuadorian Sierra. *Mountain Research and Development*, 8, 4, 331. DOI: 10.2307/3673556

HARDEN, C. 2001. Soil Erosion and Sustainable Mountain Development: Experiments, Observations, and Recommendations from the Ecuadorian Andes. *Mountain Research and Development*, 21, 1, 77-83. DOI: 10.1659/0276-4741(2001)021[0077: SEASMD]2.0. CO; 2

HARO-CARRIÓN, X., SOUTHWORTH, J. 2018. Understanding Land Cover Change in a Fragmented Forest Landscape in a Biodiversity Hotspot of Coastal Ecuador. *Remote Sensing*, 10, 12, 1980. DOI: 10.3390/rs10121980

HIDROBO, J., DA COSTA, M., PRAT, C., TRUJILLO, G., MORENO, J., ORTEGA, C. A. 2015. Sistemas de producción en áreas con cangahua habilitada en la Sierra Norte de Ecuador. *Siembra*, 2, 1, 116-127. DOI: 10.29166/siembra.v2i1.1444

HOLZ, D. J., WILLIARD, K. W. J., EDWARDS, P. J., SCHOONOVER, J. E. 2015. Soil Erosion in Humid Regions: A Review. *Journal of Contemporary Water Research & Education*, 154, 1, 48-59. DOI: 10.1111/j.1936-704X.2015.03187.x

INSTITUTO NACIONAL DE ESTADÍSTICA Y CENSOS. 2010. *Proyecciones Poblacionales. [Ecuador en Cifras]. Instituto Nacional de Estadística y Censos. INEC*. [online] [cit. 2023-03-30]. Available at: <https://www.ecuadorencifras.gob.ec/proyecciones-poblacionales/>

INSTITUTO NACIONAL DE METEOROLOGÍA E HIDROLOGÍA. 2005. *Estudio hidrológico del río Mira*. Estudios e Investigaciones Hidrológicas, 1-5.

JOKISCH, B. D. 2002. Migration and Agricultural Change: The Case of Smallholder Agriculture in Highland Ecuador. *Human Ecology*, 30, 4, 523-550. DOI: 10.1023/A: 1021198023769

KOGO, B. K., KUMAR, L., KOECH, R. 2020. Impact of Land Use/Cover Changes on Soil Erosion in Western Kenya. *Sustainability*, 12, 22, 9740. DOI: 10.3390/su12229740

KOIRALA, P., THAKURI, S., JOSHI, S., CHAUHAN, R. 2019. Estimation of Soil Erosion in Nepal Using a RUSLE Modeling and Geospatial Tool. *Geosciences*, 9, 4, 147. DOI: 10.3390/geosciences9040147

KUMAR, S., KUSHWAHA, S. P. 2013. Modelling soil erosion risk based on RUSLE-3D using GIS in a Shivalik sub-watershed. *Journal of Earth System Science*, 122, 2, 389-398. DOI: 10.1007/s12040-013-0276-0

LA MANNA, L., TARABINI, M., GOMEZ, F., ROSTAGNO, C. M. 2021. Changes in soil organic matter associated with afforestation affect erosion processes: The case of erodible volcanic soils from Patagonia. *Geoderma*, 403, 115265. DOI: 10.1016/j.geoderma.2021.115265

LETA, M. K., DEMISSIE, T. A., TRÄNCKNER, J. 2021. Modeling and Prediction of Land Use Land Cover Change Dynamics Based on Land Change Modeler (LCM) in Nashe Watershed, Upper Blue Nile Basin, Ethiopia. *Sustainability*, 13, 7, 3740. DOI: 10.3390/su13073740

LI, H., ZHU, H., QIU, L., WEI, X., LIU, B., SHAO, M. 2020. Response of soil OC, N and P to land-use change and erosion in the black soil region of the Northeast China. *Agriculture, Ecosystems & Environment*, 302, 107081. DOI: 10.1016/j.agee.2020.107081

MAETENS, W., VANMAERCKE, M., POESEN, J., JANKAUSKAS, B., JANKAUSKIENE, G., IONITA, I. 2012. Effects of land use on annual runoff and soil loss

in Europe and the Mediterranean: A meta-analysis of plot data. *Progress in Physical Geography: Earth and Environment*, 36, 5, 599-653. DOI: 10.1177/0309133312451303
MARTÍNEZ-RETURETA, R., AGUAYO, M., STEHR, A., SAUVAGE, S., ECHEVERRÍA, C., SÁNCHEZ-PÉREZ, J. M. 2020. Effect of land use/cover change on the hydrological response of a southern center basin of Chile. *Water*, 12, 1, 302. DOI: 10.3390/w12010302
MILITARY GEOGRAPHIC INSTITUTE OF ECUADOR. 2022. *Visor Geográfico Instituto Militar Ecuador*. [online] [cit. 2023-05-30]. Available at: <https://www.geoportaligm.gob.ec/portal/>
MILLWARD, A. A., MERSEY, J. E. 1999. Adapting the RUSLE to model soil erosion potential in a mountainous tropical watershed. *CATENA*, 38, 2, 109-129. DOI: 10.1016/S0341-8162(99)00067-3
MORGAN, R. P. 2009. *Soil erosion and conservation*. John Wiley & Sons.
MOSS, A. 1991. Rain impact soil crust. I. Formation on a granite derived soil. *Soil Research*, 29, 2, 271-289.
MULLIGAN, M. 1998. Modelling the geomorphological impact of climatic variability and extreme events in a semi-arid environment. *Geomorphology*, 24, 1, 59-78. DOI: 10.1016/S0169-555X(97)00101-3
NATIONAL PLANNING SECRETARY OF ECUADOR. 2013. *Sistema Nacional de Información. Sistema Nacional de Información*. [online] [cit. 2023-05-30]. Available at: <https://sni.gob.ec/coberturas>
OBIAHU, O. H., ELIAS, E. 2020. Effect of land use land cover changes on the rate of soil erosion in the Upper Eyiohia river catchment of Afikpo North Area, Nigeria. *Environmental Challenges*, 1, 100002. DOI: 10.1016/j.envc.2020.100002
OCHOA-CUEVA, P., FRIES, A., MONTESINOS, P., RODRÍGUEZ-DÍAZ, J. A., BOLL, J. 2015. Spatial Estimation of Soil Erosion Risk by Land-cover Change in the Andes OF Southern Ecuador. *Land Degradation & Development*, 26, 6, 565-573. DOI: 10.1002/ldr.2219
OZSAHIN, E., DURU, U., EROGLU, I. 2018. Land Use and Land Cover Changes (LULCC), a Key to Understand Soil Erosion Intensities in the Maritsa Basin. *Water*, 10, 3, 335. DOI: 10.3390/w10030335
PISANO, L., ZUMPANO, V., MALEK, Ž., ROSSKOPF, C. M., PARISE, M. 2017. Variations in the susceptibility to landslides, as a consequence of land cover changes: A look to the past, and another towards the future. *Science of The Total Environment*, 601-602, 1147-1159. DOI: 10.1016/j.scitotenv.2017.05.231
PULLANIKKATIL, D., PALAMULENI, L. G., RUHIIGA, T. M. 2016. Land use/land cover change and implications for ecosystems services in the Likangala River Catchment, Malawi. *Physics and Chemistry of the Earth*, Parts A/B/C, 93, 96-103. DOI: 10.1016/j.pce.2016.03.002
RAMÍREZ, F., HINCAPIÉ, E., SADEGHIAN, S. 2009. *Erodabilidad de los suelos de la zona central cafetera del departamento de Caldas*. [online] [cit. 2023-04-28]. Available at: <https://biblioteca.cenicafe.org/handle/10778/157>
RENARD, K. G. 1997. *Predicting soil erosion by water: A guide to conservation planning with the Revised Universal Soil Loss Equation (RUSLE)*. United States Government Printing.
SINGER, M. J., LE BISSONNAIS, Y. 1998. Importance of surface sealing in the erosion of some soils from a mediterranean climate. *Geomorphology*, 24, 1, 79-85. DOI: 10.1016/S0169-555X(97)00102-5
SKIDMORE, E. 1986. Wind erosion control. *Climatic change*, 9, 1, 209-218.
STADEL, C. 2005. Agricultural and settlement frontiers in the tropical Andes: The Páramo Belt of Northern Ecuador, 1960-1990. *Mountain Research and Development*, 25, 4, 386-387. DOI: 10.1659/0276-4741(2005)025[0386: AASFIT]2.0. CO; 2
STOCKING, M. 1984. Rates of erosion and sediment yield in the African environment. *IAHS-AISH publication*, 144, 285-293.

SUÁREZ DE CASTRO, F., RODRÍGUEZ GRANDAS, A. 1962. *Investigaciones sobre la erosión y la conservación de los suelos en Colombia* [Research on soil erosion and conservation in Colombia].
VANACKER, V., MOLINA, A., ROSAS, M. A., BONNESOEUR, V., ROMÁN-DAÑOBEYTIA, F., OCHOA-TOCACHI, B. F., BUYTAERT, W. 2022. The effect of natural infrastructure on water erosion mitigation in the Andes. *SOIL*, 8, 1, 133-147. DOI: 10.5194/soil-8-133-2022
VIJITH, H., HURMAIN, A., DODGE-WAN, D. 2018. Impacts of land use changes and land cover alteration on soil erosion rates and vulnerability of tropical mountain ranges in Borneo. *Remote Sensing Applications: Society and Environment*, 12, 57-69. DOI: 10.1016/j.rsase.2018.09.003
VITERI-SALAZAR, O., TOLEDO, L. 2020. The expansion of the agricultural frontier in the northern Amazon region of Ecuador, 2000-2011: Process, causes, and impact. *Land Use Policy*, 99, 104986. DOI: 10.1016/j.landusepol.2020.104986
WANG, S. W., MUNKHNASAN, L., LEE, W. K. 2021. Land use and land cover change detection and prediction in Bhutan's high altitude city of Thimphu, using cellular automata and Markov chain. *Environmental Challenges*, 2, 100017. DOI: 10.1016/j.envc.2020.100017
WISCHMEIER, W. H., SMITH, D. D. 1978. *Predicting rainfall erosion losses: A guide to conservation planning*. Department of Agriculture, Science and Education Administration.
WOO, M., FANG, G., DICENZO, P. D. 1997. The role of vegetation in the retardation of rill erosion. *CATENA*, 29, 2, 145-159. DOI: 10.1016/S0341-8162(96)00052-5
YANG, K., LU, C. 2018. Evaluation of land-use change effects on runoff and soil erosion of a hilly basin – The Yanhe River in the Chinese Loess Plateau. *Land Degradation & Development*, 29, 4, 1211-1221. DOI: 10.1002/ldr.2873
ZEBROWSKI, C., VICUÑA, A. 1997. *El cultivo de la cangahua en el medio campesino tradicional en el Ecuador*. Suelos volcánicos endurecidos (Quito, diciembre 1996), 472-481. [online] [cit. 2023-05-30]. Available at: <http://pascal-francis.inist.fr/vibad/index.php?action=getRecordDetail&idt= 2446221>
ZHANG, H., WEI, J., YANG, Q., BAARTMAN, J. E. M., GAI, L., YANG, X., LI, S., YU, J., RITSEMA, C. J., GEISSEN, V. 2017. An improved method for calculating slope length (λ) and the LS parameters of the Revised Universal Soil Loss Equation for large watersheds. *Geoderma*, 308, 36-45. DOI: https://doi.org/10.1016/j.geoderma.2017.08.006
ZHONG, Z., HAN, X., XU, Y., ZHANG, W., FU, S., LIU, W., REN, C., YANG, G., REN, G. 2019. Effects of land use change on organic carbon dynamics associated with soil aggregate fractions on the Loess Plateau, China. *Land Degradation & Development*, 30, 9, 1070-1082. DOI: 10.1002/ldr.3294
ŽONCOVÁ, M., MASNÝ, M. 2022. Comparison of land cover spatial trend model and real land cover changes: case study of Slovak Republic. *Geocarto International*, 37, 26, 13500-13517, DOI: 10.1080/10106049.2022.2082543

Vplyv zmeny využitia krajiny na eróziu pôdy v hornej a strednej časti povodia rieky Mira v Ekvádore

Súhrn

V hornej a strednej časti povodia rieky Mira v Ekvádore je predpoklad, že zmeny využitia zeme medzi rokmi 2018 – 2030 budú kopírovať trend tých, ktoré boli pozorované v rokoch 1996 – 2018. Existujú dôkazy o znížení prirodzenej pokrývky, najmä lesov a pasienkov, v porovnaní s nárastom antropických pokrývok, ako sú oblasti s poľnohospodárskymi plodinami alebo zastavané oblasti. Nebezpečným trendom je premena rôznych pokryvov na odkrytú pôdu, keďže medzi rokmi 1996 –

2018 bol dosiahnutý index zmien v tomto prípade na úrovni 185 %. Zistenia štúdie ukazujú rozsiahlu eróziu pôdy s nízkymi až vysokými hodnotami pri premene existujúcej krajinnej pokrývky, najmä z prirodzenej na antropickú a odkrytú pôdu. Vplyv odkrytej, resp. poľnohospodárskej pôdy navyše zvyšuje riziko ďalšej budúcej erózie. V rokoch 1996 až 2018 viedla zmena z lesnej na poľnohospodársku pôdu k úbytku pôdy s priemernou mierou erózie, ktorá vznikla premenou trvalých trávnych porastov a lesnej pôdy na odkrytú pôdu. V rokoch 2018 až 2030 pravdepodobný prechod z pasienkov na poľnohospodársku pôdu povedie k strate pôdy, rovnako ako zmena využitia zeme z trvalo trávnych porastov na poľnohospodársku pôdu. Tieto miery straty pôdy sú neudržateľné a oveľa vyššie ako >10 t/ha/rok, čo sa považuje za udržateľný prah.

Hornaté oblasti a lesy sú však najmenej náchylné na tieto straty. Ďalšími dominantnými príčinami pôdnej erózie v povodí sú strmé svahy a výdatné zrážky. Najvyššia pôdna erózia, sústredená do pásiem s nízkym vegetačným krytom, je v kotlinových pahorkatinách s veľkými dĺžkami svahov a strmosťou nad 60° a zrážkami s priemernými hodnotami nad 1000 mm. Hoci zrážky spúšťajú eróziu, horská geomorfológia odsúva svoju úlohu do úzadia, pretože hlavnými faktormi, ktoré generujú tieto miery erózie v povodí, sú pôdny kryt a svah. Tieto územné pomery a zmeny využívania pôdy generujú priemernú ročnú eróziu pôdy, ktorá prešla zo 14,72 t/ha/rok na 32,78 t/ha/rok a do roku 2030 pravdepodobne dosiahne 41,01 t/ha/rok. Strata prešla z 802,79 t/ha/rok v roku 1996 na 812,3 t/ha/rok v roku 2018 a do roku 2030 sa pravdepodobne zvýši na 2590,98 t/ha/rok. Tieto hodnoty patria medzi najvyššie na svete a robia z Andského údolia jeden z regiónov, ktoré strácajú a stratia najviac pôdy na planéte.

Preto je potrebné obmedziť odlesňovanie a posunúť poľnohospodársku hranicu smerom k horným oblastiam povodia, najmä pozdĺž strmých svahov, aby sa zabránilo zvýšeniu miery erózie v regióne. Nevyhnutná je obnova oblastí s obmedzeným vegetačným krytom a integrácia opatrení na ochranu pôdy s poľnohospodárskymi a pastvinárskymi činnosťami. Niektoré opatrenia na zabránenie erózie pôdy zahŕňajú nasledujúce postupy konzervačného obrábania pôdy, ochranu a hospodárenie s vodou a obnovu vegetačného krytu. Odporúčané postupy obrábania pôdy sú pásové a obrysové orezávanie, a terasy na svahovitých plochách. Regulácia pastvy vo vysokých nadmorských výškach je nevyhnutná, aby sa zabránilo zvýšenej erózii pôdy nadmerným spásaním. Hlboké obrábanie pôdy a jej úprava sa odporúčajú ako opatrenia na revitalizáciu pôdy s nízkym obsahom dusíka a organickej hmoty, kde je poľnohospodárstvo za daných podmienok nemožné (tzv. cangahua). Na obnovu degradovaných plôch a prirodzenej vegetácie sa odporúča zalesňovanie a podpora trvalých trávnych porastov. A v neposlednom rade, na obnovu erodovanej pôdy na strmých svahoch je potrebné nahradiť pestovanie plodín náchylných na eróziu lesmi.